



<b>Title</b>	Anisamide-targeted gold nanoparticles for siRNA delivery in prostate cancer - synthesis, physicochemical characterisation and in vitro evaluation
<b>Author(s)</b>	Fitzgerald, Kathleen A.; Rahme, Kamil; Guo, Jianfeng; Holmes, Justin D.; O'Driscoll, Cairtriona M.
<b>Publication date</b>	2016-03-08
<b>Original citation</b>	Fitzgerald, K. A., Rahme, K., Guo, J., Holmes, J. D. and O'Driscoll, C. M. (2016) 'Anisamide-targeted gold nanoparticles for siRNA delivery in prostate cancer - synthesis, physicochemical characterisation and in vitro evaluation', <i>Journal of Materials Chemistry B</i> , 4(13), pp. 2242-2252. doi: 10.1039/c6tb00082g
<b>Type of publication</b>	Article (peer-reviewed)
<b>Link to publisher's version</b>	<a href="http://dx.doi.org/10.1039/c6tb00082g">http://dx.doi.org/10.1039/c6tb00082g</a> Access to the full text of the published version may require a subscription.
<b>Rights</b>	© The Royal Society of Chemistry 2016. This document is the Accepted Manuscript version of a Published Work that appeared in final form in <i>Journal of Materials Chemistry B</i> . To access the final edited and published work see <a href="http://dx.doi.org/10.1039/C6TB00082G">http://dx.doi.org/10.1039/C6TB00082G</a>
<b>Item downloaded from</b>	<a href="http://hdl.handle.net/10468/5286">http://hdl.handle.net/10468/5286</a>

Downloaded on 2018-08-23T19:35:41Z



# UCC

University College Cork, Ireland  
Coláiste na hOllscoile Corcaigh

# Title Page

Anisamide-targeted Gold Nanoparticles for siRNA Delivery in Prostate Cancer – Synthesis,  
Physicochemical Characterisation and *In Vitro* Evaluation

## Author names and affiliations:

Kathleen A. Fitzgerald<sup>a</sup>

Kamil Rahme<sup>b,c,d</sup>

Jianfeng Guo<sup>a</sup>

Justin D. Holmes<sup>c,d</sup>

Caitriona M. O’Driscoll\*<sup>a</sup>

<sup>a</sup>*Pharmacodelivery Group, School of Pharmacy, University College Cork, Ireland*

<sup>b</sup>*Department of Sciences, Faculty of Natural and Applied Science, Notre Dame University  
(Louaize), Lebanon*

<sup>c</sup>*Materials Chemistry and Analysis Group, Department of Chemistry and the Tyndall  
National Institute, University College Cork, Cork, Ireland*

<sup>d</sup>*AMBER (Advanced Materials and Biological Engineering Research Centre), CRANN  
(Centre for Research on Adaptive Nanostructures and Nanodevices), Trinity College Dublin,  
Dublin, Ireland*

## \*Corresponding author:

Prof. Caitriona O’Driscoll, Cavanagh Pharmacy Building, School of Pharmacy, College  
Road, University College Cork, Cork, Ireland.

Tel: +35321490 1396.

Fax: +353 21 490 1656

Email: [caitriona.odriscoll@ucc.ie](mailto:caitriona.odriscoll@ucc.ie) (Caitriona M. O’Driscoll)

## 24 **Abstract**

25 Metastatic prostate cancer is a leading cause of cancer-related death in men and current  
26 chemotherapies are largely inadequate in terms of efficacy and toxicity, hence improved  
27 treatments are required. The application of siRNA as a cancer therapeutic holds great  
28 promise. However, translation of siRNA into the clinic is dependent on the availability of an  
29 effective delivery system. Gold nanoparticles (AuNPs) are known to be effective and non-  
30 toxic siRNA delivery agents. In this study, a stable gold nanosphere coated with  
31 poly(ethylenimine) (PEI) was prepared to yield PEI capped AuNPs (Au-PEI). The PEI was  
32 further conjugated with the targeting ligand anisamide (AA, is known to bind to the sigma  
33 receptor overexpressed on the surface of prostate cancer cells) to produce an anisamide-  
34 targeted nanoparticle (Au-PEI-AA). The resulting untargeted and targeted nanoparticles (Au-  
35 PEI and Au-PEI-AA respectively) were positively charged and efficiently complexed siRNA.  
36 Au-PEI-AA mediated siRNA uptake into PC3 prostate cancer cells via binding to the sigma  
37 receptor. In addition, the Au-PEI-AA.siRNA complexes resulted in highly efficient  
38 knockdown of the RelA gene (~ 70 %) when cells were transfected in serum-free medium. In  
39 contrast, no knockdown was observed in the presence of serum, suggesting that adsorption of  
40 serum proteins inhibits the binding of the anisamide moiety to the sigma receptor. This study  
41 provides (for the first time) proof of principle that anisamide-labelled gold nanoparticles can  
42 target the sigma receptor. Further optimisation of the formulation to increase serum stability  
43 will enhance its potential to treat prostate cancer.

## 44 1 Introduction

45 Prostate cancer is expected to be the second-leading cause of cancer-related death in men in  
46 the US in 2015 <sup>1</sup>. Despite improvements in the treatments available for prostate cancer,  
47 particularly relating to patients who have developed metastatic ‘castrate resistant’ disease,  
48 current therapies can offer only limited increases in lifespan <sup>2</sup>. Because of this there is an  
49 urgent need to develop improved therapies for those whose prostate cancer has developed to  
50 this stage <sup>3</sup>. As a consequence of the increased understanding of the genetic changes within  
51 the cell which can contribute to the development and spread of prostate cancer <sup>4</sup>, small  
52 interfering RNA (siRNA) has been investigated for the treatment of prostate cancer with very  
53 promising results <sup>5, 6</sup>. siRNA can regulate gene expression by binding specifically to  
54 corresponding mRNA molecules. These mRNA molecules are then blocked from undergoing  
55 the normal process of translation into protein or, alternatively, are degraded in the cytoplasm  
56 <sup>7</sup>.

57 Although siRNA has potential to treat human diseases, there are major obstacles impeding  
58 the *in vivo* application of such therapy <sup>4</sup>. The major barrier to the use of siRNA therapy in the  
59 clinic is delivery <sup>8</sup>. Naked siRNA duplexes are highly unstable, especially in the serum,  
60 demonstrate extremely low cellular uptake and transfection efficiencies, and may induce  
61 immune system activation following systemic administration<sup>9-11</sup>. Delivery systems or  
62 ‘vectors’ formulated as nanoparticles have been used to protect siRNA in the circulation and  
63 to ensure cellular uptake after administration. Theoretically, following systemic  
64 nanoparticulate siRNA delivery *in vivo*, any cell within the body can be transfected. This may  
65 result in harmful consequences to healthy cells <sup>12</sup> and lead to the requirement for higher  
66 amounts of siRNA to be administered to achieve therapeutic efficacy. Therefore, the

67 incorporation of a targeting ligand into the delivery vector to facilitate site-specific delivery  
68 to target tissues and cells is critical for success <sup>13</sup>.

69 Among the range of nanoparticulate delivery vector systems under investigation are gold  
70 nanoparticles (AuNPs) which can be readily functionalised and are capable of delivering both  
71 small drug molecules and large biomolecules, such as proteins, DNA and RNA <sup>14</sup>. The gold  
72 core can be easily modified to yield cationic AuNPs which complex siRNA via electrostatic  
73 interaction <sup>15</sup>. The ability of cationic AuNPs to bind siRNA, protect it from enzymatic  
74 degradation and mediate gene silencing has been reported previously <sup>16</sup>.

75 The aim of this project was to develop an anisamide-labelled AuNP for targeted delivery of  
76 siRNA which binds to the sigma receptor that is overexpressed on the surface of prostate  
77 cancer cells. The gold was functionalised with PEI to give a cationic AuNP capable of  
78 binding siRNA (Au-PEI). To mediate specific uptake in prostate cancer cells, the PEI coating  
79 was modified with the anisamide-ligand (Au-PEI-AA). The resulting Au-PEI-AA  
80 nanoparticle was assessed for its capacity to complex siRNA, to facilitate receptor-mediated  
81 endocytosis and to silence genes in both the absence and presence of serum in sigma receptor  
82 positive PC3 prostate cancer cells.

## 83 **2 Materials/Methods**

### 84 **2.1 Reagents**

85 All materials were purchased from Sigma unless otherwise stated. Negative control non-  
86 silencing siRNA (sense strand sequence 5'-UUC UCC GAA CGU GUC ACG U-3') was  
87 purchased from Sigma (Wicklow, Ireland). The same sequence modified with 6FAM on the  
88 3' end of the sense strand was used for fluorescence experiments (Sigma, Wicklow, Ireland).  
89 RelA siRNA (sense strand sequence 5'-CCAUCAACUAUGAUGAGUU-3') was purchased  
90 from IDT (Coralville, Iowa, U.S.A.). Purified H<sub>2</sub>O (resistivity  $\approx$  18.2 M $\Omega$  cm) was used as a  
91 solvent for the synthesis of AuNPs. All glassware was cleaned with aqua regia (3 parts of  
92 concentrated HCl and 1 part of concentrated HNO<sub>3</sub>), rinsed with distilled water, ethanol and  
93 acetone, and oven-dried before use.

### 94 **2.2 Synthesis of AuNPs**

#### 95 **2.2.1 UV-visible Spectroscopy**

96 Optical absorption spectra were obtained on a CARY UV–visible spectrophotometer with a  
97 Xenon lamp (190–900 nm range, 0.5 nm resolution).

#### 98 **2.2.2 Scanning Electron Microscopy (SEM)**

99 AuNPs were deposited from solution onto a Si wafer and air-dried prior to analysis using a  
100 FEI 630 NanoSEM equipped with an Oxford INCA energy dispersive X-ray (EDX) detector  
101 operated at 5 kV.

#### 102 **2.2.3 Attenuated-Total-Reflection Infrared Spectroscopy (ATR-IR)**

103

104 ATR-IR spectra were collected on a Nicolet 6700 Infrared Spectrometer equipped with a  
105 VariGATR (Harrick Scientific) and a liquid N<sub>2</sub> cooled MgCdTe (MCT) detector. The  
106 samples were mounted on a KBr disc and spectra were collected under p-polarization at a  
107 grazing angle of 65 ° using 1000 cumulative scans with a resolution of 2 cm<sup>-1</sup>.

#### 108 **2.2.4 NMR**

109 <sup>1</sup>H (600 MHz) and <sup>13</sup>C (150.9 MHz) NMR spectra were recorded on a Bruker Avance III 600  
110 NMR spectrometer using a Bruker 5mm Dual C-H Cryoprobe operating at 17 K with a  
111 sample temperature of 300 K. All spectra were recorded in deuterated dimethylsulfoxide  
112 (DMSO-d<sub>6</sub>) using trimethylsilylpropanoic acid (TSP) as an internal chemical shift reference  
113 standard.

#### 114 **2.2.5 Synthesis of Gold Nanoparticles Capped with PEI**

115 1 ml PEI (2.3 mmol L<sup>-1</sup>) was added to 203 ml of HAuCl<sub>4</sub>·3H<sub>2</sub>O (0.25 mmol L<sup>-1</sup>) under  
116 stirring at room temperature (RT); the colour of the solution changed from pale yellow to  
117 deep yellow. On addition of 0.71 ml of L-ascorbic acid (100 mmol L<sup>-1</sup>) the colour of the  
118 solution turned red within 5 s. The solution was kept under stirring at RT overnight to obtain  
119 Au-PEI NPs.

#### 120 **2.2.6 Synthesis of NHS-activated Anisic Acid**

121 EDC.HCl (1.5 eq, 1.9 g, 9.9 mmol) was added to a solution of anisic acid (1 g, 6.572 mmol)  
122 in dry DCM (250 ml) under Argon, followed by N-hydroxysuccinimide (NHS) (1.45 eq, 1.1  
123 g, 9.56 mmol). The reaction mixture was stirred for approximately 42 h under Argon at RT.  
124 The organic phase was washed twice with water followed by a wash with brine, dried over  
125 magnesium sulfate (MgSO<sub>4</sub>), filtered on whatman filter paper and evaporated. The activated  
126 ester thus obtained was left to stir in 30 ml dry pentane for approximately 48 h. It was

127 filtered, dried under vacuum and used without further purification. The anisic-NHS ester  
128 yield was approximately 90 %. The product was analysed using FTIR and NMR  
129 spectroscopy.

### 130 **2.2.7 Synthesis of Anisamide-targeted Gold Nanoparticles (Au-PEI-AA)**

131 250  $\mu$ l of NaOH 0.1 M was added to 25 ml of pre-synthesized  $\sim$  60 nm Au-PEI NPs ( $\sim$  0.25  
132 mmol L<sup>-1</sup>-11.2  $\mu$ mol L<sup>-1</sup>), followed by the addition of 0.5 ml of anisic-NHS (25 mg/ml) in dry  
133 DMSO and the solution was left under stirring for 21 h at RT to achieve Au-PEI-AA NPs.  
134 The resulting Au-PEI-AA solution was purified using centrifugation at 12,000 rpm for 15  
135 min and the free anisic-NHS in the supernatant was quantified using a CARY UV-Vis  
136 spectrophotometer with a Xenon lamp (190-900 nm range, 0.5 nm resolution).

### 137 **2.3 Cell Culture**

138 PC3 human prostate cancer cells (European Collection of Cell Cultures (ECACC)) were  
139 cultured in RPMI-1640 media supplemented with 10 % Fetal Bovine Serum (FBS), 2 mM L-  
140 Glutamine, 50 units/ml penicillin and 50  $\mu$ g/ml streptomycin<sup>17</sup>. Cells were maintained in a  
141 humidified, 5 % CO<sub>2</sub> tissue culture incubator at 37 °C.

### 142 **2.4 Preparation of Gold:siRNA Complexes**

143 To complex siRNA, Au-PEI and Au-PEI-AA were mixed at the required Au:siRNA mass  
144 ratio (MR) in water and incubated at RT for 30 min at 300 rpm on a thermomixer.

### 145 **2.5 Gel Retardation Assay**

146 The ability of AuNPs to complex siRNA was assessed using gel retardation<sup>15</sup>.  
147 Nanocomplexes were prepared at various MRs of Au:siRNA up to MR 10. Samples were  
148 then mixed with 1x Blue Juice Gel loading buffer (Invitrogen, U.S.A.) and loaded onto a 1 %  
149 (w/v) agarose gel containing SafeView<sup>TM</sup> (NBS Biologicals Ltd, England) (6  $\mu$ l/100 ml).



150 Each well contained 0.5  $\mu\text{g}$  siRNA and naked siRNA (uncomplexed by AuNPs) was used as  
151 a control. Electrophoresis was carried out at 120 V for 30 min with a Tris-borate-EDTA  
152 buffer. The resulting gel was photographed under UV light.

## 153 **2.6 Size and Charge Measurements**

154 Particle Z-average size and charge were measured using dynamic light scattering (DLS) and  
155 electrophoretic mobility measurements respectively using the Malvern Zetasizer Nano ZS <sup>15</sup>.  
156 AuNP.siRNA complexes were prepared at MR 7.5 (as detailed in section 2.4) to a final  
157 volume of 1 ml. Each sample contained 20  $\mu\text{g}$  gold. Three readings of Z-average size (nm),  
158 polydispersity and zeta potential (mV) were taken at 25°C using the default non-invasive  
159 back scattering (NIBS) technique with a detection angle of 173 °.

## 160 **2.7 Competitive Uptake**

161 To investigate if cellular uptake of the nanocomplexes was mediated via binding of the  
162 anisamide moiety to the sigma receptor, competitive uptake following pre-incubation with  
163 haloperidol was undertaken <sup>5</sup>. PC3 cells were seeded  $1 \times 10^5$  cells/well in 24-well plates 24 h  
164 prior to transfection. Before transfection, cells were pre-treated with 50  $\mu\text{M}$  haloperidol for 3  
165 h. Control cells were incubated with fresh media without haloperidol. Au-PEI and Au-PEI-  
166 AA were complexed with fluorescent siRNA at MR 7.5. Complexes (final volume 125  
167  $\mu\text{l}$ /well in water) were added to cells in serum-free and antibiotic-free media (375  $\mu\text{l}$ /well).  
168 Control cells were incubated in 375  $\mu\text{l}$  transfection media and 125  $\mu\text{l}$  water. Naked siRNA  
169 samples were prepared by diluting siRNA to 125  $\mu\text{l}$ /well in water and were added to 375  $\mu\text{l}$   
170 transfection media. Fluorescent siRNA complexed with Lipofectamine 2000 ® (Invitrogen)  
171 was prepared as per manufacturer's instruction. Transfection was carried out over 4 h using  
172 50 nM siRNA. After this time period, cells were incubated with 200  $\mu\text{l}$  CellScrub™  
173 (Genlatins) for 15 min to remove uninternalised complexes from the cell surface <sup>6</sup>. They were

174 then washed twice with pre-warmed PBS and detached from plates using 200  $\mu$ l 0.25x  
175 Trypsin (15 min, 37°C). Cells were centrifuged at 1000 rpm for 5 min (4 °C) and washed  
176 with 1 ml cold PBS. They were centrifuged again at 1000 rpm for 5 min (4 °C) and  
177 resuspended in 700  $\mu$ l cold PBS in Polystyrene Round-Bottom Tubes (Becton  
178 Dickinson). The fluorescence associated with 10,000 cells was measured with a FACS Caliber  
179 instrument (BD Bioscience) and the data was analysed using the Cell Quest Pro software.

## 180 **2.8 Intracellular Fate of Targeted AuNPs**

181 To investigate the time course of Au-PEI-AA.siRNA uptake and intracellular distribution, co-  
182 localisation with the endolysosomal compartment was investigated 30 min and 4 h post-  
183 transfection<sup>5</sup>. PC3 prostate cancer cells were seeded 5 x 10<sup>4</sup> cells/well in 12-well culture  
184 plates with glass bottoms (MatTek™). After 48 h, Au-PEI-AA was complexed with siRNA at  
185 MR 7.5. Cells were transfected with 100 nM fluorescent siRNA for 30 min or 4 h in serum-  
186 free media. At the end of the transfection period, late endosomes and lysosomes were labelled  
187 using 75 nM LysoTracker Deep Red (Molecular Probes, Invitrogen) in RPMI-1640 for 30  
188 min at 37 °C. Cells were washed with PBS and analysed using an Olympus FV 1000 confocal  
189 microscope. Fluorescent siRNA was detected using excitation at 488 nm and LysoTracker  
190 Deep Red was detected using excitation at 633 nm.

## 191 **2.9 Toxicity of AuNPs**

192 Cytotoxicity of AuNP.siRNA complexes was assessed using the MTT assay with 3-(4, 5-  
193 dimethylthiazol-2-yl)-2, 5-diphenyltetrazolium bromide<sup>18</sup>. PC3 prostate cancer cells were  
194 seeded 1 x10<sup>4</sup> cells/well 24 h prior to transfection in 96-well plates. siRNA (200 nM) or  
195 AuNP.siRNA complexes were added to cells in both serum-containing and serum-free media  
196 for 24 h. siRNA complexed with Lipofectamine 2000® was prepared as per manufacturer's  
197 instructions. After 24 h, the media was replaced with 100  $\mu$ l RPMI-1640 and 20  $\mu$ l MTT (5

198 ml/ml solution in PBS) and incubated at 37 °C for 4 h. The supernatant was removed and the  
199 formazon crystals were dissolved in 100 µl DMSO. Absorbance was measured at 570 nm  
200 using a UV plate reader.

## 201 **2.10 Gene Knockdown**

202 The RelA unit of Nuclear Factor κB (NF-κB) was selected as a prostate cancer-relevant gene  
203 for gene knockdown experiments<sup>3</sup>. PC3 cells were seeded 5 x 10<sup>4</sup> cells/well in 24 well plates  
204 24 h prior to transfection. AuNPs were complexed with negative control non-silencing  
205 siRNA or RelA siRNA at MR 7.5. Lipofectamine 2000 ® formulations were prepared as per  
206 manufacturer's instructions. Transfection was carried out over 24 h using 200 nM siRNA in  
207 both serum-containing and serum-free media. At the end of the transfection period, cells were  
208 lysed and RNA was extracted using GenElute™ Mammalian Total RNA Miniprep Kit  
209 (Sigma) as per manufacturer's instructions. First-strand complementary DNA (cDNA) was  
210 generated from the total RNA using a High Capacity cDNA Reverse Transcription Kit  
211 (Applied Biosystems). Gene expression was assessed by real-time qPCR using the Applied  
212 Biosystem's Real Time PCR System (Model 7300). Cycling conditions were as follows: 10  
213 min (min) at 95 °C, 40 cycles of [15 s (sec) at 95 °C; 1 min at 60 °C]. Assays were performed  
214 using appropriate primer sets for RelA (catalogue number Hs01042010\_m1) and 18S  
215 (catalogue number Hs99999901\_s1) (Taqman ®, Applied Biosystems). The quantitative level  
216 of each RelA mRNA was measured as a fluorescent signal corrected according to the signal  
217 for 18S mRNA. The 2-delta Ct method was used to quantify the relative changes in mRNA  
218 <sup>19</sup>.

## 219 **2.11 Cellular Uptake in Absence/Presence of Serum**

220 Both flow cytometry and fluorescent microscopy were used to assess nanoparticle uptake in  
221 the absence and presence of serum proteins.

222 For flow cytometry analysis, PC3 cells were seeded  $1 \times 10^5$  cells/well in 24-well plates 24 h  
223 prior to transfection. AuNPs were complexed with fluorescent FAM-siRNA at MR 7.5.  
224 Complexes were added to cells as detailed in section 2.7. Transfection was carried out over  
225 24 h using 50 nM siRNA and samples were prepared for flow cytometry analysis as  
226 previously outlined in section 2.7. The fluorescence associated with 10,000 cells was  
227 measured with a FACS Caliber instrument (BD Bioscience) and the data was analysed using  
228 the Cell Quest Pro software.

229 In addition, for microscopy analysis PC3 cells were seeded  $1 \times 10^5$  cells/well 24 h prior to  
230 transfection. AuNPs complexed with FAM-siRNA at MR 7.5 were added to cells.  
231 Transfection was carried out over 4 h using 100 nM siRNA in both serum-containing and  
232 serum-free media. After this time period, cells were incubated for 15 mins with CellScrub™  
233 and washed twice with PBS. Samples were imaged in PBS using an Olympus IX70 inverted  
234 microscope (exciter filter BP470-490, barrier filter BA515).

## 235 **2.12 Serum Stability**

236 In order to investigate the stability of siRNA alone and in complexation with AuNPs, siRNA  
237 (0.5 µg) or AuNP.siRNA complexes were incubated for different time intervals in 10 % (v/v)  
238 FBS at 37 °C<sup>20</sup>. Following incubation at 4, 8 and 24 h, the serum was inactivated by heating  
239 the sample to 80 °C for 5 min. Samples were then stored at -20 °C until ready for analysis by  
240 gel electrophoresis. Samples included at time 0 were prepared with 10% FBS which was  
241 previously heat deactivated by heating at 80 °C for 5 mins. All samples were then treated  
242 with excess heparin (2000 I.U./ml in PBS) for 1 h at RT. Samples were mixed with 1x Blue  
243 Juice Gel loading buffer and loaded onto a 1.5 % (w/v) agarose gel containing SafeView™ (6  
244 µl/100 ml). Electrophoresis was carried out at 120 V for 30 min with a Tris-borate-EDTA  
245 buffer. The resulting gel was photographed under UV light.

246 In addition, the effect of serum on the particle size of AuNPs was investigated by incubating  
247 AuNPs in 10 % FBS for 4 h at 37 °C<sup>18</sup>. Following this, size measurements were carried out  
248 by DLS. Each 1ml sample contained 20 µg gold.

### 249 **2.13 Statistical Analysis**

250 One-way analysis of variance (ANOVA) was used to compare multiple groups followed by  
251 Bonferroni's post hoc test. In **Figure 5** and **Figure 10** two-way ANOVA was used to  
252 compare treatment groups followed by Bonferroni's post hoc test. Statistical significance is  
253 displayed as \*P<0.05, \*\*P<0.01, \*\*\*P<0.001.

## 254 3 Results/Discussion

### 255 3.1 Anisamide-targeted AuNPs

256 As gene delivery vectors AuNPs have a number of advantages including good  
257 biocompatibility and ease of synthesis <sup>21</sup>. In this study, gold nanospheres were used as a  
258 scaffold to prepare an anisamide-targeted siRNA delivery vector for use in prostate cancer  
259 (**Figure 1**). Firstly, AuNPs were chemically modified with PEI during the synthesis (Au-  
260 PEI). PEI was used because it is a cationic polymer that is known for its capacity to complex  
261 negatively charged siRNA molecules. Furthermore, after nanoparticulate endocytosis, the pH  
262 of the endosome falls and PEI becomes protonated resulting in increased osmotic pressure in  
263 the endosome. This facilitates osmotic swelling, endosomal rupture and release of siRNA into  
264 the cytoplasm where it can exert its effect <sup>22</sup>. The gold core was specifically modified with  
265 low molecular weight ( $M_w$ ) PEI (2kDa). Higher  $M_w$  PEIs (e.g. 10 kDa, 70 kDa) are known to  
266 give better transfection rates <sup>23</sup> but cannot be metabolised by cellular enzymes and therefore  
267 are more toxic <sup>24</sup>. In addition, strong binding of high  $M_w$  PEIs to nucleic acids can result in  
268 poor intracellular release and reduced efficiency <sup>24</sup>. In this study, the purpose of the PEI was  
269 to facilitate siRNA binding to the gold nanoparticle and subsequent intracellular release.  
270 Hence, non-toxic low  $M_w$  PEI was used. The Au-PEI nanoparticle was conjugated directly  
271 with pre-activated anisamide (Anisic-NHS ester) to prepare an anisamide-targeted AuNP  
272 (Au-PEI-AA). The targeting ligand anisamide is known to bind specifically to the sigma  
273 receptor which is over-expressed on the surface of prostate cancer cells <sup>5, 25</sup>. The untargeted  
274 control was prepared in the same way but without the conjugation of anisamide (Au-PEI)  
275 (**Figure 1**).

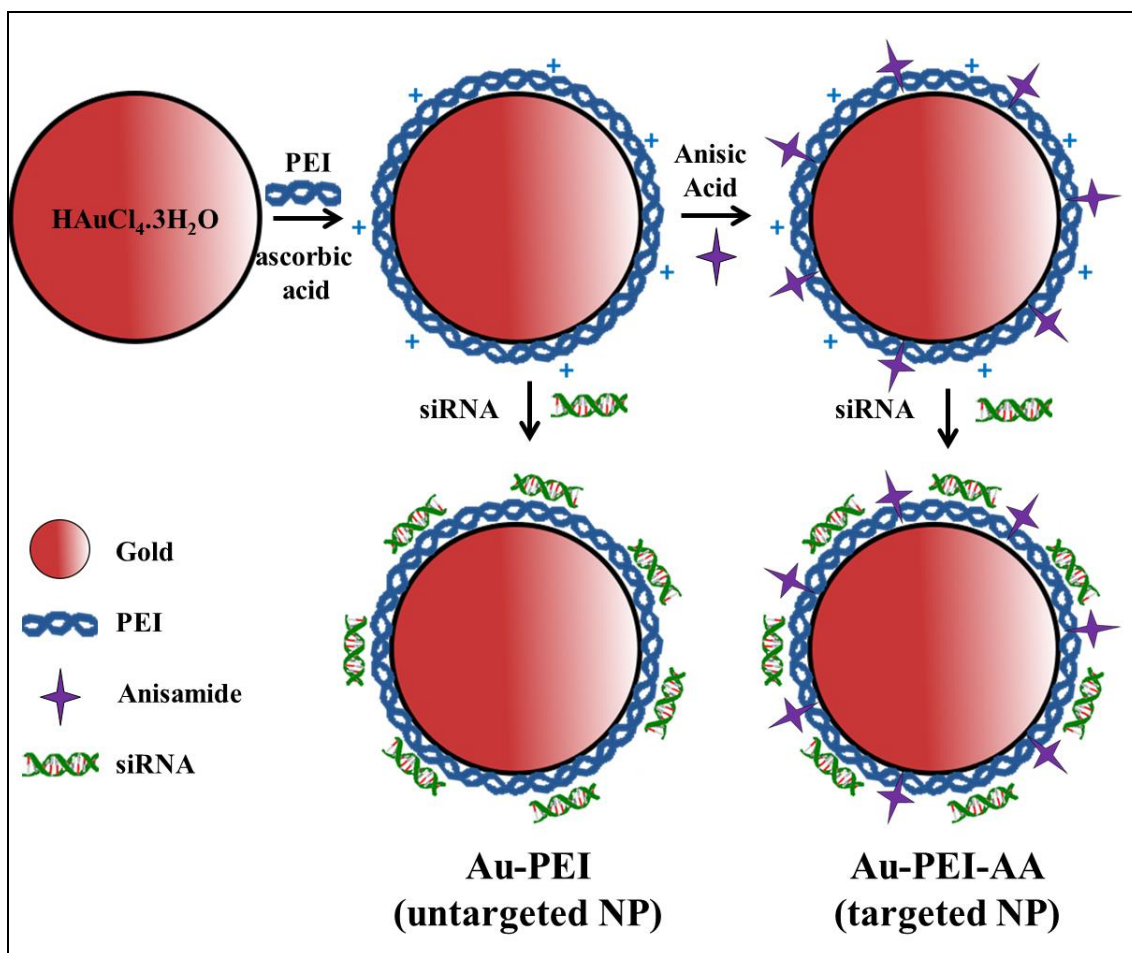


**Figure 1**

Schematic showing the untargeted (Au-PEI) and targeted (Au-PEI-AA) AuNPs. The AuNP core was first coated with cationic PEI during its synthesis. The PEI was then chemically conjugated with anisamide and complexed with siRNA to form the targeted Au-PEI-AA nanoparticle. The untargeted counterpart (Au-PEI) was prepared in the same way but without the conjugation with anisamide on the cationic PEI surface.

### 276 3.2 Synthesis and Characterization of Au-PEI

277 Most studies using PEI capped gold nanoparticles (Au-PEI) utilise a slow (at RT) or a fast  
 278 (high temperature) auto reduction of  $\text{HAuCl}_4 \cdot 3\text{H}_2\text{O}$  by addition of excess PEI (used  
 279 simultaneously as reductant and stabilizer)<sup>16, 26, 27</sup>. In this study, a simple and direct reduction  
 280 of  $\text{HAuCl}_4 \cdot 3\text{H}_2\text{O}$  precursor in the presence of PEI (2 kDa) with ascorbic acid at RT was used  
 281 to synthesise Au-PEI NPs<sup>28</sup>. On addition of a small amount of PEI to  $\text{HAuCl}_4$  the colour of  
 282 the solution changed from light to deep yellow indicating the formation of a complex  
 283 between the amino groups of the PEI and the Au metal ions. The addition of ascorbic acid

284 reduced the Au ions into Au (0) and the PEI capped Au-PEI NPs formed quickly (within 5  
 285 seconds) as indicated by the change in colour of the solution to red<sup>15, 29, 30</sup>. The UV-Vis  
 286 spectrum showed that the resulting nanoparticles possessed an absorption band with a  
 287 wavelength centred at approximately 534 nm (**Figure 2 (a)**) due to the surface plasmon  
 288 resonance band of AuNPs. SEM analysis showed the nanoparticles were spherical in shape  
 289 with an average gold core diameter of about  $52 \pm 8$  nm as analysed using *Image J* software  
 290 (**Figure 2(b)** and (c)). However, the overall average size of the nanoparticle dispersion  
 291 obtained from DLS measurements in water was slightly larger (Z-average size  $67 \pm 2$  nm,  
 292 polydispersity index (PDI)  $0.12 \pm 0.01$ ), with a positive Zeta Potential ( $31 \pm 1$  mV) (**Table 1**).  
 293 This confirmed that AuNPs were successfully coated with PEI. It is worth noting that the Au-  
 294 PEI NP was stable for more than two month at 4 °C.

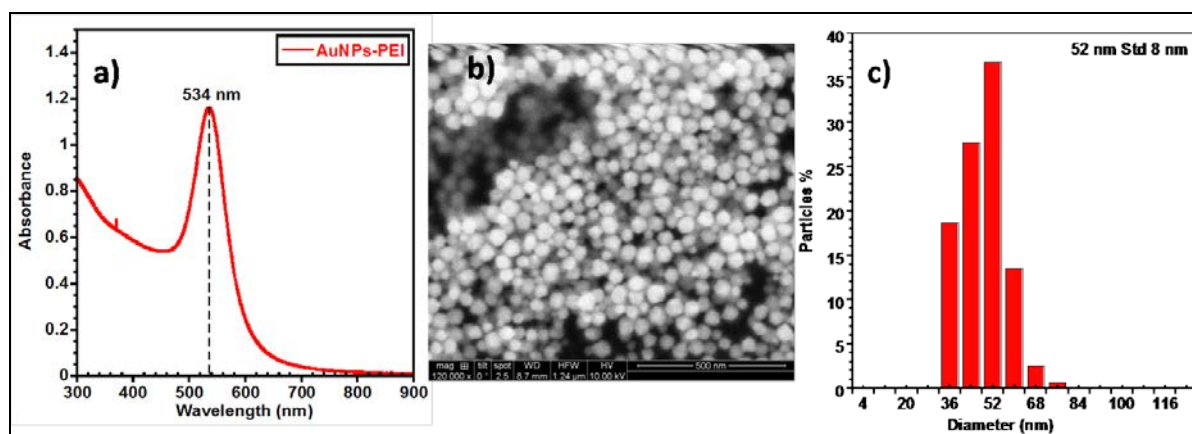


**Figure 2**

(a) UV-vis spectrum of the obtained Au-PEI NPs; (b) SEM image of Au-PEI (scale bar = 500 nm); (c) size of Au-PEI ( $52 \pm 8$  nm) analysed from SEM images using *Image J* software (more than 500 nanoparticles were counted and their size was determined).

### 295 3.3 Synthesis and Characterisation of Anisamide-targeted Au-PEI-AA

296 The anisic acid was activated by reacting with NHS to form an anisic-NHS ester which could  
 297 react with the amino groups of PEI in water to form a stable amide linkage. This resulted in  
 298 the formation of Au-PEI-AA NPs. The successful activation of the anisic acid was confirmed  
 299 with FTIR and NMR analysis as presented in supporting information. **Figure S1** shows the



300 ATR-FTIR spectrum of the anisic acid, NHS and anisic-NHS product. It is evident from this  
301 spectrum that the product is very different from the starting material with shifted bands  
302 supporting its formation. The purity (~ 95 %) and formation of the product anisic-NHS was  
303 also confirmed by  $^1\text{H}$  and  $^{13}\text{C}$  NMR analysis (Results not shown).

304 The synthesis of AuNPs-PEI-AA (**Figure 1**) was adapted from a method previously  
305 described by Xu et al <sup>31</sup> where fluorescein was attached onto gadolinium oxide NPs capped  
306 with PEI. In this study the amines of PEI were reacted with NHS-activated anisic acid. The  
307 attachment of anisic acid-NHS onto the Au-PEI surface did not show a significant change in  
308 the initial red colour of the gold solution nor the average size distribution, while the zeta  
309 potential was found to decrease slightly by ~ 5 mV ( $p < 0.01$ ) after attachment of AA (**Table**  
310 **1**). To confirm the attachment of anisic acid onto Au-PEI NPs, UV-vis spectroscopy was  
311 used. The nanoparticles were collected by centrifugation and redispersed in water. The UV-  
312 vis spectrum (**Figure 3**) showed a band at ~ 265 nm for Au-PEI-AA NPs. Furthermore, UV-  
313 vis allowed us to quantify the anisic acid-NHS left in solution after centrifugation of the Au-  
314 PEI-AA NPs. Results indicated that ~ 50 % (~ 35  $\mu\text{mol L}^{-1}$ ) of the initially added anisic acid  
315 was grafted onto the Au-PEI surface as shown (**Figure S2**).

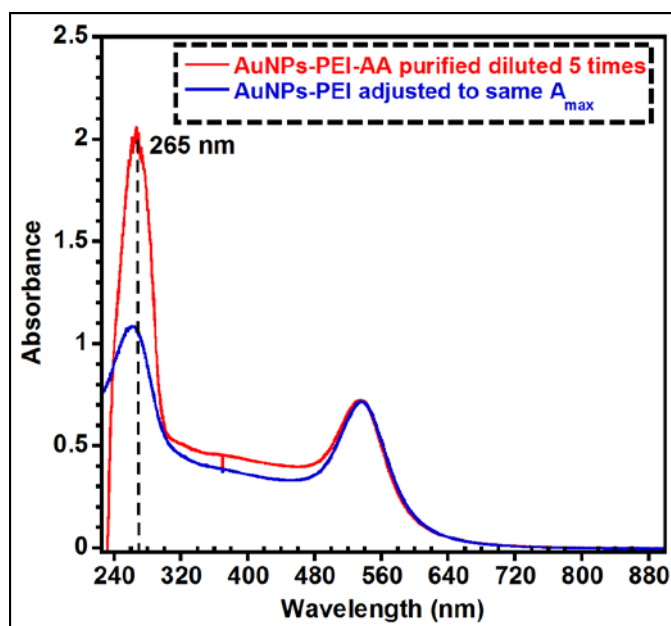


**Figure 3**

UV-vis spectra of the obtained Au-PEI and Au-PEI-AA after purification (centrifugation and redispersion in water) diluted 5 times and adjusted to the same  $A_{\max}$ .

316

### 317 3.4 Agarose Gel Binding and Physicochemical Characterisation

318 Cationic delivery vectors complex siRNA via electrostatic interaction with negatively  
 319 charged phosphates on the siRNA backbone<sup>32</sup>. The ability of Au-PEI and Au-PEI-AA to  
 320 complex siRNA at different MRs was monitored by gel retardation. As show in **Figure 4**, the  
 321 untargeted Au-PEI fully complexed siRNA even at the lowest MR tested. In contrast, the  
 322 targeted Au-PEI-AA did not fully complex siRNA until MR 7.5. For Au-PEI-AA, the  
 323 conjugation of PEI with the anisamide-targeting moiety caused some degree of steric  
 324 interference significantly reducing the siRNA binding capacity. Hence a higher MR of  
 325 Au:siRNA was required to fully complex siRNA. Thus in further studies, a constant MR 7.5  
 326 of Au:siRNA was used for both untargeted and targeted nanoparticles.

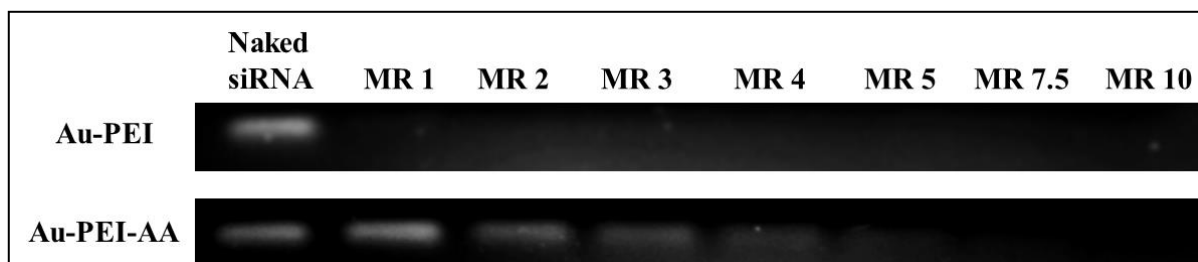


**Figure 4**

Binding gel of untargeted (Au-PEI) and targeted (Au-PEI-AA) AuNPs (MR = mass ratio Au:siRNA). Full complexation was evident for the Au-PEI at all mass ratios tested. Full complexation occurred at MR 7.5 for Au-PEI-AA.

327

328 Particle size and surface charge are key parameters that affect the *in vivo* efficacy of  
 329 nanoparticles for gene delivery. DLS was used to assess the size of Au-PEI and Au-PEI-AA  
 330 both prior to and after complexation with siRNA. As shown in **Table 1** nanoparticle diameter  
 331 was unaffected by the addition of siRNA to the formulation (both Au-PEI and Au-PEI-AA).  
 332 Au-PEI-AA had a slightly lower particle diameter (Au-PEI-AA 62.8 nm versus Au-PEI 69.8  
 333 nm) possibly due to tighter packing of the PEI caused by the hydrophobic nature of the  
 334 anisamide-targeting moiety. However, both AuNPs were within a suitable size range for  
 335 exploiting the ‘enhanced permeability and retention (EPR) effect’ for passively targeting the  
 336 ‘leaky’ vasculature of solid tumours<sup>33</sup>.

siRNA	Size (nm)		Charge (+mV)		PDI	
	-	+	-	+	-	+
Au-PEI	69.8 (± 1.1)	69.9 (± 1.1)	33.8 (± 0.3)	31.3 (± 0.8)	0.154 (± 0.004)	0.119 (± 0.002)
Au-PEI-AA	62.8 (± 0.8)	65.6 (± 0.9)	27.6 (± 0.7)	24.5 (± 2.0)	0.393 (± 0.011)	0.293 (± 0.003)

**Table 1**

Average nanoparticle size (nm), charge (mV) and polydispersity index (PDI) of untargeted (Au-PEI) and targeted (Au-PEI-AA) nanoparticles. Samples were prepared to contain 20 µg gold at a mass ratio Au:siRNA of 7.5 and measured in water at 25 °C. (n=3, mean ± S.D.).

337 The targeted nanoparticle had a slightly lower surface charge relative to the untargeted  
338 nanoparticle (+27.6 mV versus +33.8 mV) possibly due to the conjugation of free PEI amines  
339 to create the anisamide-targeting moiety. There was a trend toward reduced surface charge  
340 following complexation with siRNA by ~2.5-3 mV for both the untargeted and targeted  
341 nanoparticles due to charge neutralisation by anionic siRNA. Furthermore, the polydispersity  
342 index (PDI), which gives an indication as to the uniformity of nanoparticle size, was below  
343 0.4 for all samples indicating only a small variation in nanoparticle diameter<sup>34</sup>.

### 344 **3.5 Prostate Cancer Cellular Uptake**

345 Recently, a variety of anisamide-targeted delivery vectors have been developed to  
346 specifically target the sigma receptor that is known to be over-expressed on the surface of  
347 prostate cancer cells<sup>5, 25, 35</sup>. To investigate if the anisamide-targeted AuNPs facilitates siRNA  
348 uptake into prostate cancer cells, the sigma receptor positive prostate cancer PC3 cell line  
349 was used<sup>5</sup>. Haloperidol, a known sigma receptor antagonist, is known to competitively  
350 inhibit anisamide-mediated uptake into sigma receptor positive cells<sup>5, 25, 36</sup> and was used to  
351 investigate receptor-mediated uptake. As shown in **Figure 5**, despite a high cationic surface  
352 charge, the untargeted Au-PEI nanoparticle had poor uptake into prostate cancer cells with or  
353 without haloperidol pre-treatment further reinforcing the poor ability of low M<sub>w</sub> PEI to  
354 mediate cell transfection<sup>23</sup>. In contrast, the targeted Au-PEI-AA nanoparticle resulted in a  
355 high percentage of fluorescent-positive cells indicating successful transfection. As the only  
356 difference between the untargeted and targeted nanoparticle was the presence of the  
357 anisamide moiety, the high level of uptake gave a strong indication that the targeted  
358 nanoparticle was taken into cells via receptor-mediated endocytosis by binding to the sigma  
359 receptor. This uptake mechanism was confirmed by the finding that cellular siRNA uptake  
360 was significantly reduced following haloperidol pre-treatment of cells (P<0.001) (**Figure 5**)<sup>5</sup>.

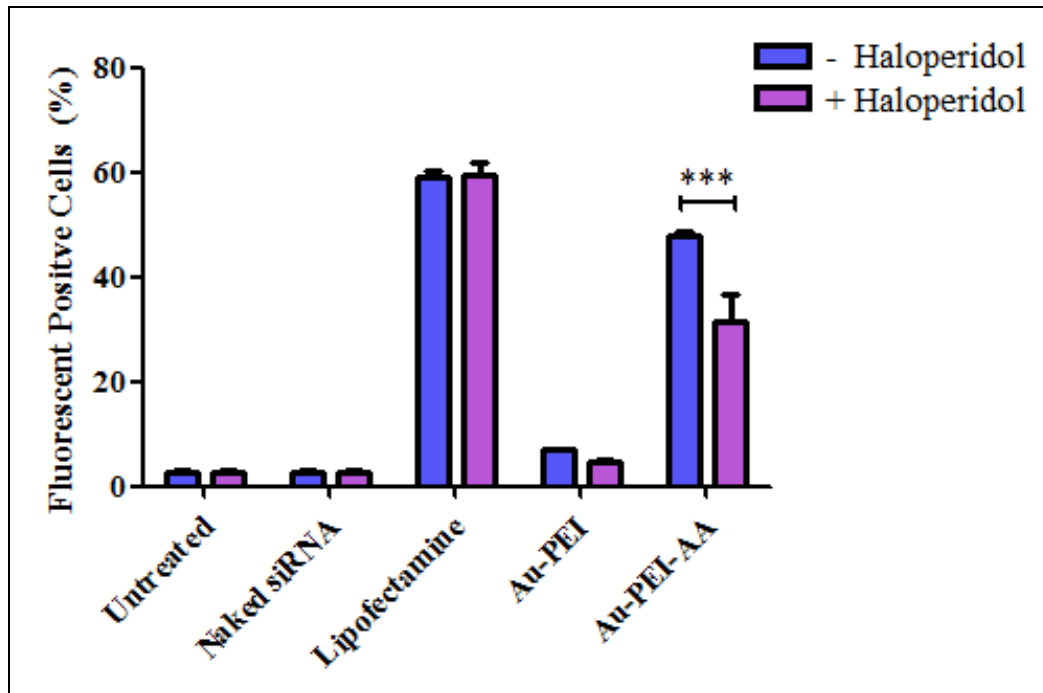


**Figure 5**

AuNP cellular uptake into sigma receptor-positive PC3 prostate cancer cells. Transfection to investigate competitive uptake of AuNPs was carried out following 3 h pre-incubation with 50  $\mu$ M haloperidol. Cells were then incubated with Au-PEI and Au-PEI-AA complexed with FAM-siRNA (50 nM) for 4 h and cell uptake was measured using flow cytometry (n=3, mean  $\pm$  S.D.). (\*\*\*)P<0.001).

### 361 **3.6 Intracellular Fate**

362 PEI is known to be highly efficient in facilitating endosomal escape after cellular uptake by a  
 363 process termed the ‘proton sponge effect’ whereby the fall in pH in the endosome protonates  
 364 PEI leading to increased osmotic pressure and endosomal rupture<sup>37</sup>. In order to visualise the  
 365 intracellular trafficking of FAM-labelled siRNA with Au-PEI-AA, the endosome was  
 366 labelled using LysoTracker Deep Red. Cells were visualised at 30 min and 4 h to determine  
 367 the subcellular location of siRNA at these time points.

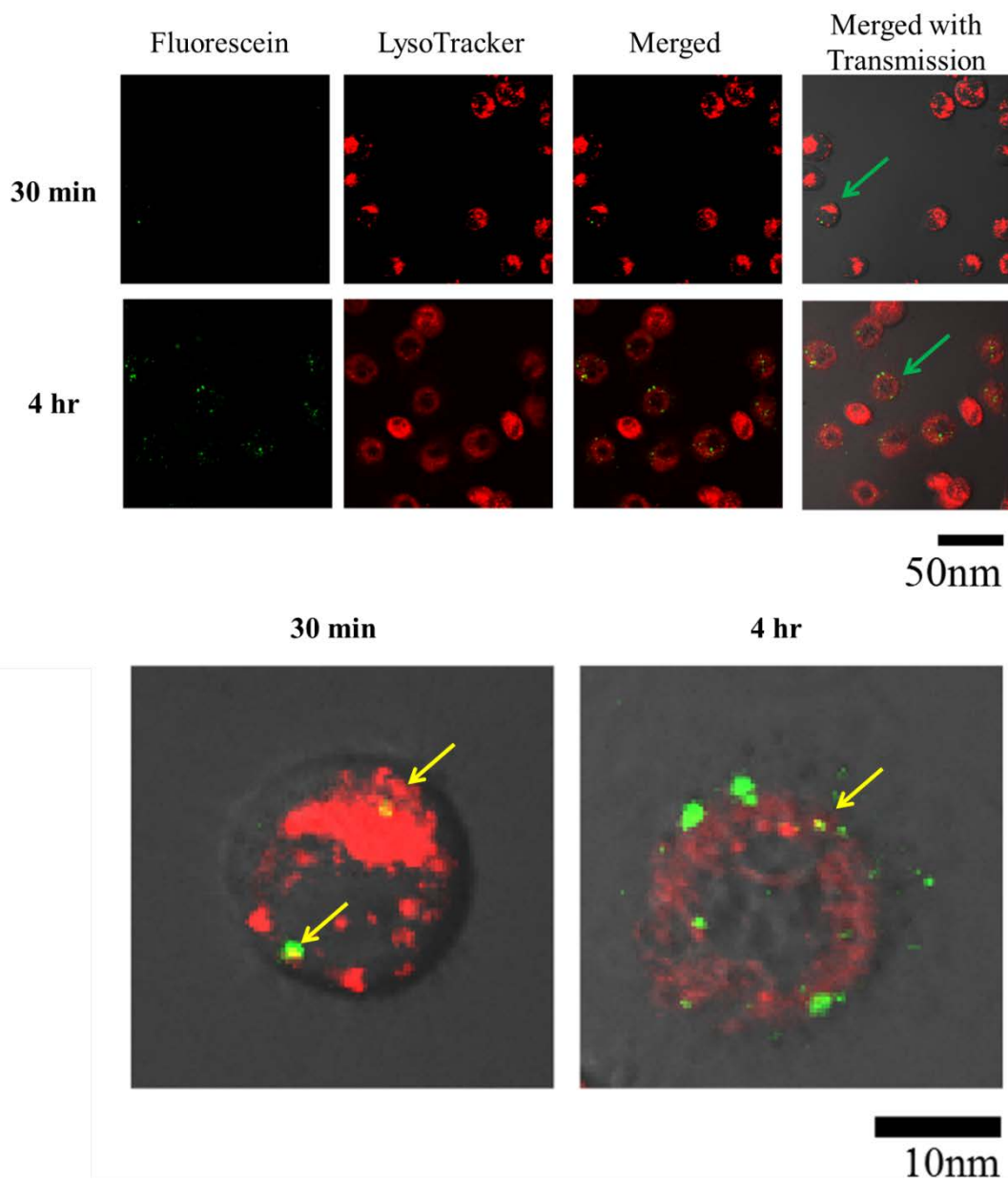


**Figure 6**

Uptake of Au-PEI-AA complexed with FAM-siRNA into PC3 prostate cancer cells at 30 min and 4 h. (a) Confocal microscopy images demonstrating the intracellular fate following nanoparticle uptake. Left to right: FAM-siRNA, LysoTracker Deep Red, merged fluorescent images and merged fluorescent images including transmission. Green arrow indicates specific cells that were further magnified in (b). (b) Magnification of selective cells demonstrating subcellular location 30 min and 4 h post-transfection. Yellow arrow indicates co-localisation of siRNA with endosome. siRNA was fluorescently labelled (green) and the endosome was labelled using LysoTracker (red).

368 30 min after transfection there was little FAM-siRNA cellular uptake as demonstrated by the  
 369 low level of green fluorescence visible within cells (**Figure 6 (a)**). However, when one of the  
 370 siRNA-fluorescent-positive cells was magnified at this time point it was apparent that the  
 371 formulation facilitated highly efficient endosomal escape (**Figure 6 (b)**). Even at this early  
 372 time point some green fluorescent siRNA was visible in the cytoplasm of the cell following  
 373 escape from the endosomal compartment. However, some fluorescent siRNA was also visible  
 374 in the endolysosomes of the cell as apparent from the yellow staining resulting from the co-  
 375 localisation between the siRNA and LysoTracker Deep Red (yellow arrow, **Figure 6(b)**).

376 At 4 h after transfection, much higher levels of siRNA are visible within the cell (**Figure 6**  
 377 **(a)**) consistent with high cellular uptake of the targeted nanoparticle. At this time point the  
 378 majority of siRNA had escaped from the endosome and was detected in the cytoplasm where  
 379 it can exert its mechanism of action (**Figure 6 (b)**)<sup>27</sup>.

### 380 3.7 Cytotoxicity

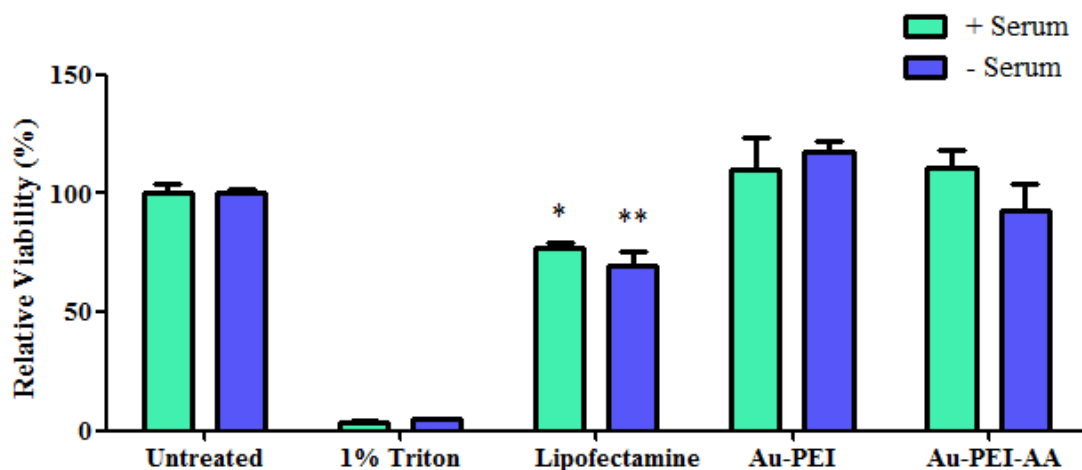


**Figure 7**

PC3 prostate cancer cell viability 24 h post-transfection with complexes at MR 7.5 of Au:siRNA (200 nM siRNA) in the presence and absence of serum. Cell viability was measured using the MTT assay and absorbance values were normalised to the untreated control (n=3, mean  $\pm$  S.D.). (\*  $P < 0.05$ , \*\*  $P < 0.01$  reduction in cell viability relative to untreated control).

381 AuNPs are generally recognised as non-toxic delivery vectors<sup>38</sup>. However, the modification  
382 of AuNPs with PEI can result in increased cell toxicity, reportedly due to the presence of  
383 unbound cationic PEI in the aqueous solution which elicits more cell toxicity<sup>27</sup>. Furthermore,  
384 a cationic surface charge on AuNPs, as is present on both Au-PEI and Au-PEI-AA  
385 formulations used in this study, may impact upon cellular toxicity<sup>39, 40</sup>. It is essential that  
386 delivery vectors for siRNA gene therapy in cancer are non-toxic to cancerous cells. In  
387 contrast the toxicity should come from the RNAi effects of the siRNA and not from the  
388 nanocarrier itself<sup>41</sup>. Hence the MTT assay was used to assess the impact of Au-PEI and Au-  
389 PEI-AA formulations on cell toxicity. Serum is frequently included in cell culture media as it  
390 provides essential growth factors and hormones to facilitate cell growth<sup>42</sup>. It also acts as a  
391 detoxification agent<sup>42</sup> whereby serum proteins bind to the nanoparticle surface and shield  
392 cells from the toxic surface coating<sup>43</sup>. Hence the cytotoxicity of AuNPs both in the presence  
393 and absence of serum was investigated.

394 Both Au-PEI and Au-PEI-AA nanoparticles proved to be non-toxic using 200 nM siRNA  
395 (**Figure 7**) at 24 h both in the presence and absence of serum. In contrast, the commercially-  
396 available cationic lipid vector Lipofectamine 2000® significantly reduced cell viability in  
397 both the presence ( $P < 0.05$ ) and absence ( $P < 0.01$ ) of serum. Thus these AuNPs are suitable  
398 for investigating therapeutic gene knockdown in the PC3 prostate cancer cell line.

### 399 **3.8 Gene Knockdown**

400 In order to investigate the gene knockdown potential of both Au-PEI and Au-PEI-AA  
401 formulations in the presence and absence of serum, AuNPs were complexed with siRNA  
402 targeting the RelA subunit of the NF- $\kappa$ B transcription factor<sup>44</sup>. The constitutive activation of  
403 this transcription factor is implicated in a variety of cancer types, including prostate cancer,  
404 where it leads to the transcription of a diverse range of genes including those associated with



405 proliferation, metastases and angiogenesis<sup>3</sup>. Having established the nanoparticles were non-  
406 toxic at 24 h using 200 nM siRNA, this time point and siRNA concentration were used to  
407 investigate gene knockdown.

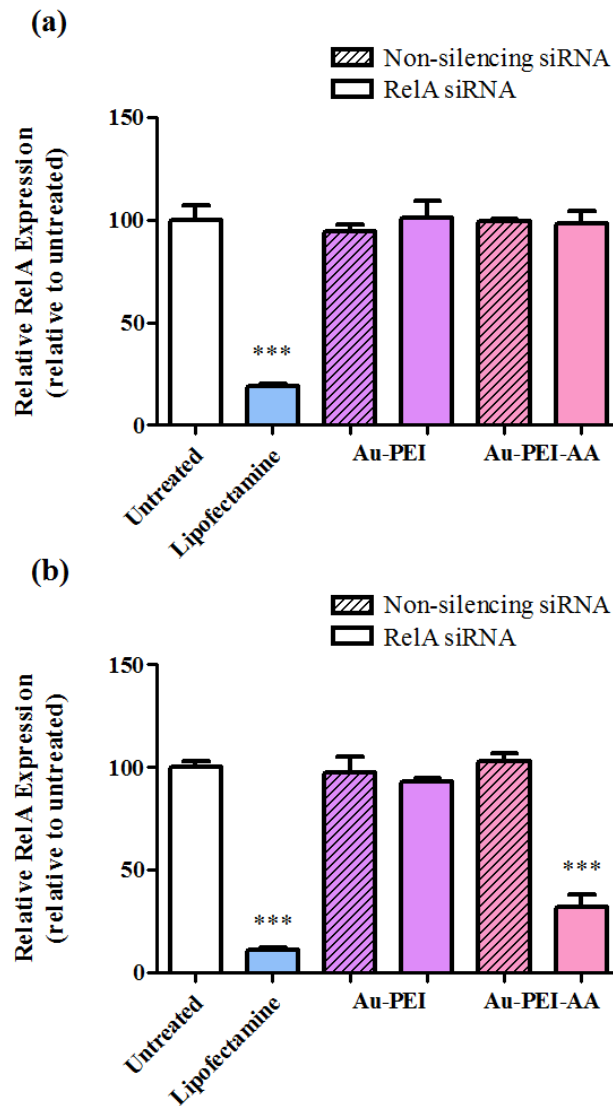


**Figure 8**

Gene knockdown using AuNPs. (a) In serum-containing media. (b) In serum-free media. Knockdown of the RelA gene was quantified 24 h post-transfection with 200 nM siRNA. Negative control non-silencing siRNA was used as a control. (n=3, mean  $\pm$  S.D.) (\*\*\*) $P < 0.001$  relative to untreated control).

408 As demonstrated in **Figure 8 (a)**, both the untargeted and targeted nanoparticles were unable  
409 to mediate RelA gene knockdown in serum-containing media. In contrast, the targeted  
410 nanoparticle mediated highly significant gene knockdown (~ 70 %) in serum-free transfection  
411 conditions (**Figure 8 (b)**) ( $P < 0.001$ ). Although the commercially available vector  
412 Lipofectamine mediated higher levels of gene knockdown relative to Au-PEI-AA in the  
413 absence of serum, it was toxic to cells and would be unsuitable as a gene delivery vector *in*  
414 *vivo* (**Figure 7**). The difference in gene knockdown mediated by Au-PEI-AA in the presence  
415 and absence of serum was then further investigated.

### 416 3.9 Nanoparticle Uptake in the Absence and Presence of Serum

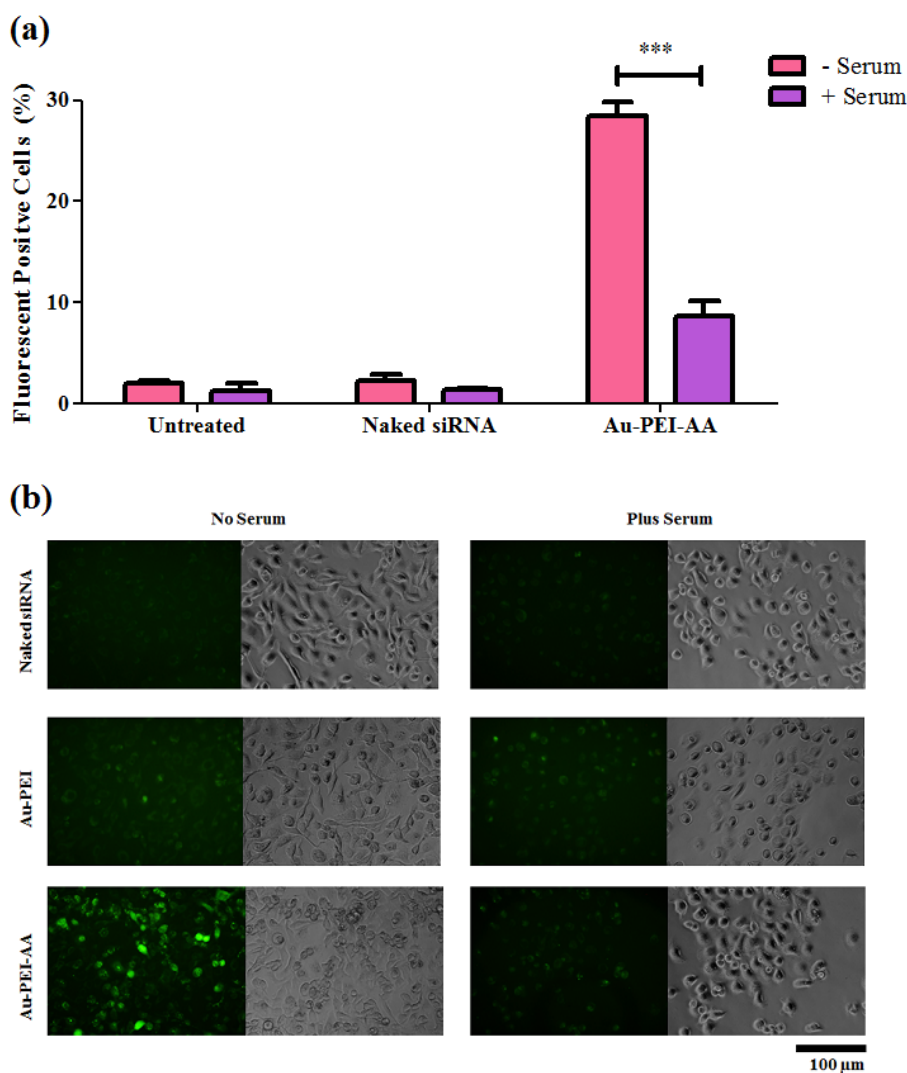


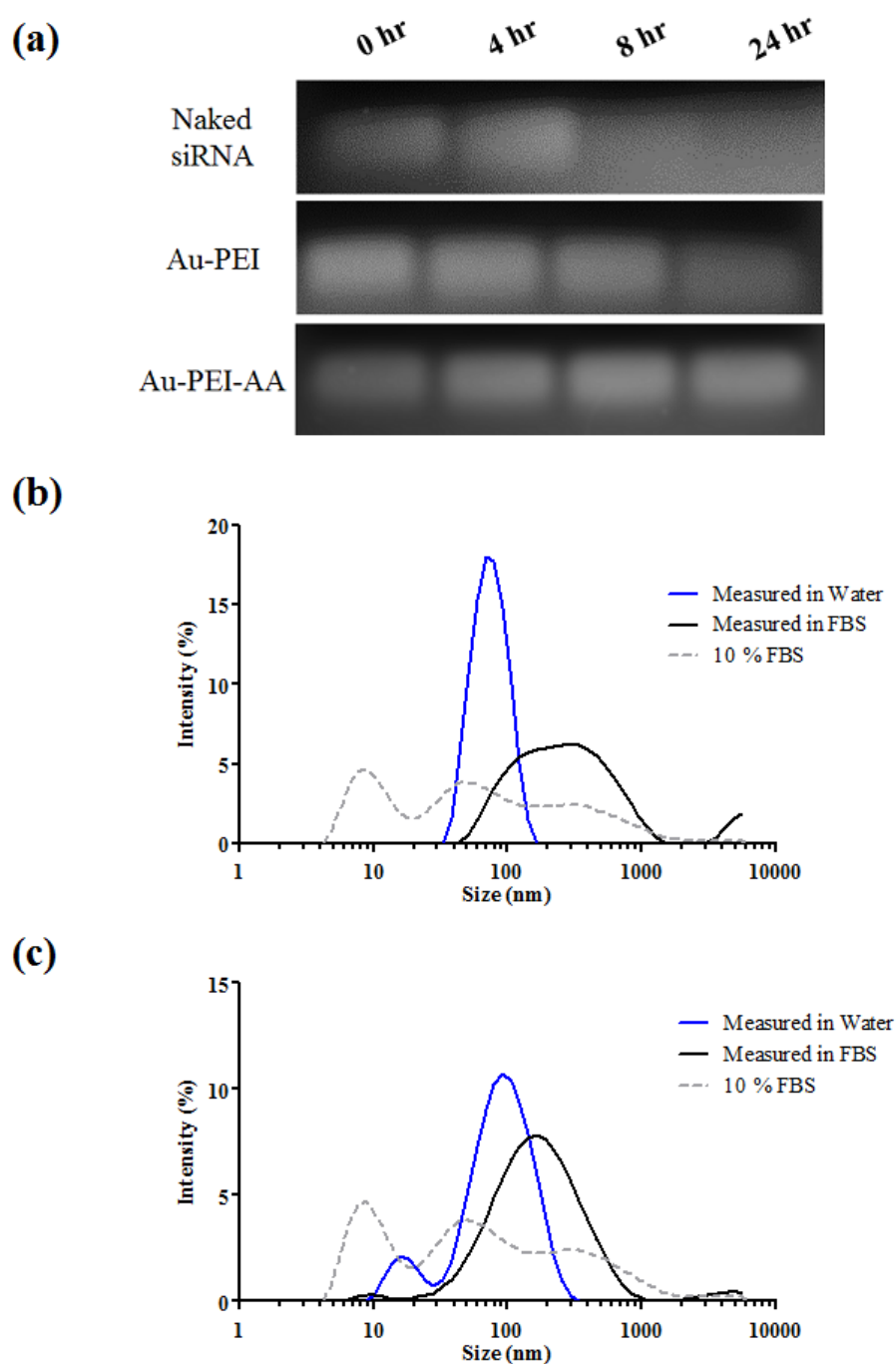
### Figure 9

AuNP cellular uptake into PC3 prostate cancer cells in the absence and presence of serum. (a) 24 h uptake of 50 nM FAM-siRNA complexed with Au-PEI-AA as measured by flow cytometry (n=3, mean  $\pm$  S.D.). (b) 4 h uptake of 100 nM FAM-siRNA complexed with Au-PEI and Au-PEI-AA visualised by microscopy. (\*\*\*)P<0.001).

417 The uptake of fluorescent siRNA complexed with Au-PEI-AA was investigated using flow  
418 cytometry in the absence and presence of serum. As show in **Figure 9 (a)**, uptake of Au-PEI-  
419 AA was significantly reduced in the presence of serum. This result indicates that the lack of  
420 transfection by the targeted nanoparticle as shown in **Figure 8 (a)** was indeed the result of  
421 poor siRNA cellular uptake in the presence of serum.

422 This result was further corroborated using fluorescent microscopy whereby PC3 cells were  
423 imaged 4 h post-transfection with fluorescent siRNA in the absence and presence of serum  
424 (**Figure 9 (b)**). Au-PEI had poor cellular uptake which was unaffected by the presence of  
425 serum. In contrast and similar to the results displayed in **Figure 9 (a)**, the uptake of  
426 fluorescent siRNA complexed with Au-PEI-AA was reduced in serum-containing  
427 transfection conditions (P<0.001).

428 Thus having established that serum proteins inhibited siRNA uptake when complexed with  
429 the targeted nanoparticle, two possible explanations were possible; (a) serum proteins may  
430 have displaced siRNA from the surface of AuNPs resulting in poor cellular uptake, or (b)  
431 binding of serum proteins to the targeted nanoparticle complexed with siRNA may have  
432 shielded the anisamide-targeting moiety on the surface of AuNPs thus inhibiting the receptor-  
433 targeting ability of the formulation. In order to identify the most likely mechanism the serum  
434 stability of the nanoparticles was investigated.

**Figure 10**

AuNP stability in serum. (a) Serum stability of siRNA following up to 24 h incubation in 10 % FBS (naked or complexed with Au-PEI or Au-PEI-AA). (b) Particle size measurements of Au-PEI after incubation for 4 h in water or 10% serum. (c) Particle size measurements of Au-PEI-AA after incubation for 4 h in water or 10% serum.

436 The stability of siRNA complexed with Au-PEI and Au-PEI-AA in 10 % FBS was  
437 investigated as previously employed using gel retardation after incubation at 37 °C for 24 h  
438 <sup>20</sup>. The results demonstrated that both Au-PEI and Au-PEI-AA protected siRNA from serum-  
439 induced degradation for up to 24 h (**Figure 10(a)**). This result not only indicates that the  
440 nanoparticles were successful in protecting siRNA from degradation, but it also indicates that  
441 serum proteins do not displace siRNA from the surface of the nanoparticles. If displacement  
442 occurred, the siRNA would most likely be degraded by serum nucleases as occurred for  
443 naked siRNA (**Figure 10 (a)**).

444 It is widely reported that negatively charged serum proteins in FBS can adsorb onto the  
445 cationic surface of nanoparticles <sup>43, 45</sup>. To confirm this interaction occurs with the AuNPs in  
446 this study, particle size was measured in water and in 10 % serum following incubation at 37  
447 °C for 4 h. The particle diameters of both Au-PEI (**Figure 10 (a)**), and Au-PEI-AA (**Figure**  
448 **10 (b)**) increased following incubation in FBS relative to water (average diameter untargeted  
449 213.9 nm versus 68.54 nm; targeted: 125.6 nm versus 66.5 nm). This increase in particle size  
450 is indicative of non-specific protein binding to the surface of the nanoparticle <sup>34</sup>. Previously  
451 such interactions have been reported to improve the transfection efficacy of AuNPs <sup>46</sup>. This  
452 has been attributed to the ability of adsorbed serum proteins to stabilise nanoparticles against  
453 aggregation in electrolytic solutions <sup>43</sup>. However, it is evident in this study that the adsorption  
454 of serum proteins has the opposite effect on transfection by these nanoparticles. The  
455 anisamide-functionalised Au-PEI-AA nanoparticles appear to lose their targeting ability to  
456 access the sigma receptor on PC3 cells due to shielding of the ligand by adsorbed serum  
457 proteins. Hence further modification of the Au-PEI-AA is necessary to increase *in vivo*  
458 activity, where serum is present. The incorporation of poly(ethylene glycol) (PEG) chains  
459 into formulations have been widely reported to stabilise particles against nonspecific binding

460 of proteins <sup>47</sup>. The option to modify the formulation of the AuNPs with PEG will be the focus  
461 of future work.

## 462 **4 Conclusion**

463 In conclusion an anisamide-targeted AuNP using low M<sub>w</sub> PEI to complex siRNA was  
464 successfully synthesised and tested in PC3 prostate cancer cells. Uptake of Au-PEI-  
465 AA.siRNA was competitively reduced after pre-incubation with haloperidol proving that  
466 uptake occurred via binding to the sigma receptor. The PEI present in Au-PEI-AA mediated  
467 highly efficient endosomal escape. Both Au-PEI and Au-PEI-AA nanoparticles were non-  
468 toxic up to 200 nM siRNA in the presence and absence of serum. Au-PEI-AA mediated  
469 highly efficient RelA gene knockdown but only in serum-free transfection conditions. While  
470 this is the first time that the anisamide-targeting moiety has been successfully utilised to  
471 target AuNPs to prostate cancer cells, further modification of the formulation is required to  
472 avoid interaction with serum proteins and thus to enhance the potential for *in vivo*  
473 application.

## 474 **5 Acknowledgements**

475 This project is supported by the Irish Cancer Society Project Grant PCI11ODR. We  
476 acknowledge financial support from Science Foundation Ireland and AMBER (Grant  
477 12/RC/2278) and the Irish Research Council, for a Government of Ireland Postdoctoral  
478 Fellowship to Jianfeng Guo (GOIPD/2013/150). The authors would like to acknowledge the  
479 Department of Anatomy & Neuroscience Imaging Centre, BioSciences Institute, University  
480 College Cork, for assistance in preparing and imaging specimens for this research.

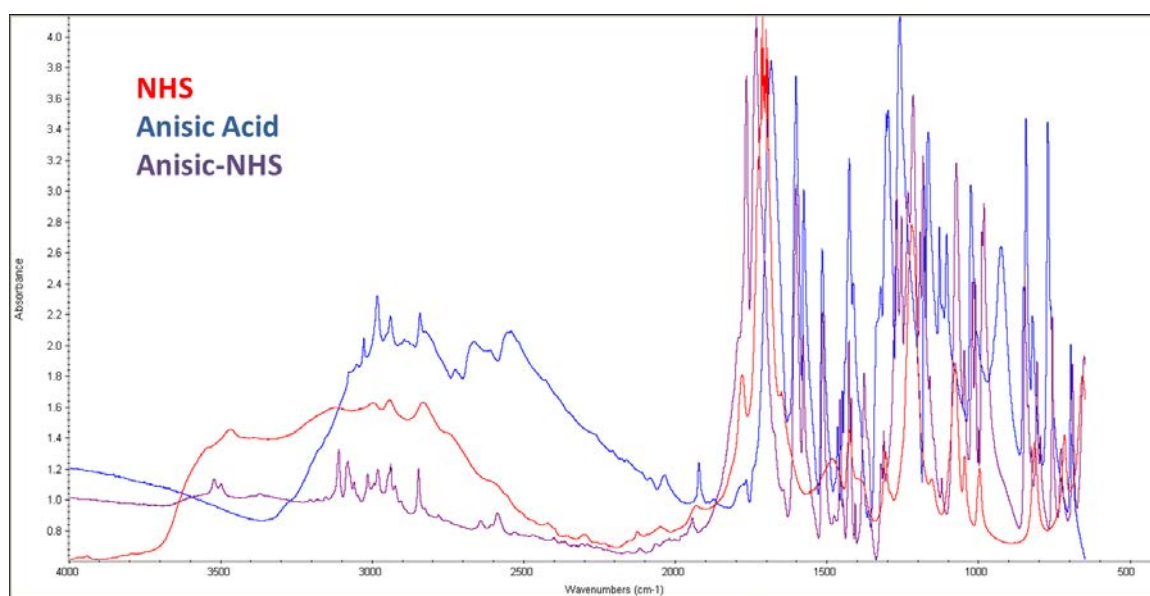


**Figure S1.** ATR-IR spectra of the anisic acid, NHS and the obtained product activated anisic-NHS Ester

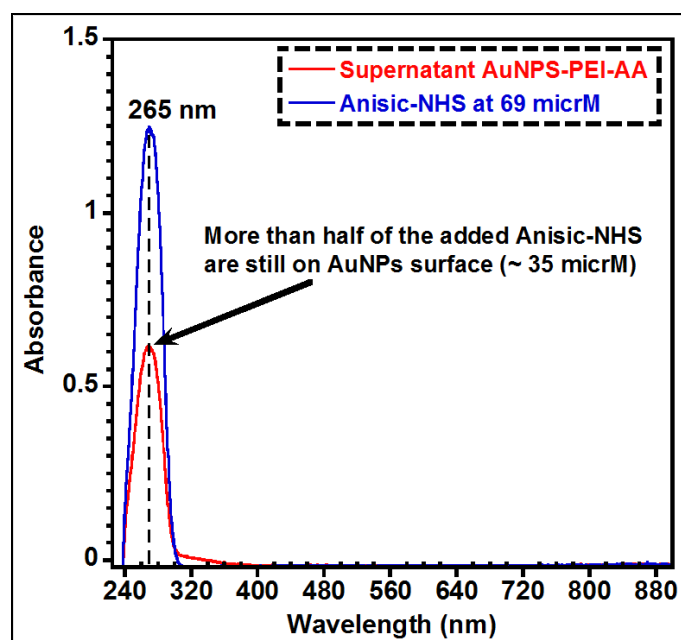


**Figure S2.** UV-vis absorption spectra of anisic-NHS. In order to verify that NHS activated anisic acid was attached onto Au-PEI, the resultant colloidal solution was centrifuged at 12,000 rpm at RT for 15 min. The anisic-NHS in the supernatant (red) was analysed using



UV-visible spectroscopy. When compared to anisic-NHS prepared using a concentration of 69  $\mu\text{M}$  (blue, a concentration for the reaction initially), results indicated that more than 50% of anisic-NHS had been grafted onto Au-PEI.

483 **7 References**

- 484 1. R. L. Siegel, K. D. Miller and A. Jemal, *CA: a cancer journal for clinicians*, 2015, **65**,  
485 5-29.
- 486 2. J. N. Graff and E. D. Chamberlain, *Core evidence*, 2015, **10**, 1-10.
- 487 3. K. A. Fitzgerald, J. C. Evans, J. McCarthy, J. Guo, M. Prencipe, M. Kearney, W. R.  
488 Watson and C. M. O'Driscoll, *Expert opinion on therapeutic targets*, 2014, **18**, 633-  
489 649.
- 490 4. J. F. Guo, L. Bourre, D. M. Soden, G. C. O'Sullivan and C. O'Driscoll, *Biotechnol*  
491 *Adv*, 2011, **29**, 402-417.
- 492 5. J. Guo, J. R. Ogier, S. Desgranges, R. Darcy and C. O'Driscoll, *Biomaterials*, 2012,  
493 **33**, 7775-7784.
- 494 6. J. F. Guo, W. P. Cheng, J. X. Gu, C. X. Ding, X. Z. Qu, Z. Z. Yang and C. O'Driscoll,  
495 *Eur J Pharm Sci*, 2012, **45**, 521-532.
- 496 7. J. Guo, J. C. Evans and C. M. O'Driscoll, *Trends in molecular medicine*, 2013, **19**,  
497 250-261.
- 498 8. K. A. Whitehead, R. Langer and D. G. Anderson, *Nature Reviews Drug Discovery*,  
499 2009, **8**, 129-138.
- 500 9. S. Choung, Y. J. Kim, S. Kim, H. O. Park and Y. C. Choi, *Biochem Bioph Res Co*,  
501 2006, **342**, 919-927.
- 502 10. H. R. Kim, I. K. Kim, K. H. Bae, S. H. Lee, Y. Lee and T. G. Park, *Mol Pharm*, 2008,  
503 **5**, 622-631.
- 504 11. S. Jung, S. H. Lee, H. Mok, H. J. Chung and T. G. Park, *Journal of Controlled*  
505 *Release*, 2010, **144**, 306-313.
- 506 12. J. Guo, K. A. Fisher, R. Darcy, J. F. Cryan and C. O'Driscoll, *Molecular bioSystems*,  
507 2010, **6**, 1143-1161.
- 508 13. Y. Ikeda and K. Taira, *Pharmaceutical research*, 2006, **23**, 1631-1640.
- 509 14. P. Ghosh, G. Han, M. De, C. K. Kim and V. M. Rotello, *Advanced drug delivery*  
510 *reviews*, 2008, **60**, 1307-1315.
- 511 15. J. F. Guo, M. J. Armstrong, C. M. O'Driscoll, J. D. Holmes and K. Rahme, *Rsc Adv*,  
512 2015, **5**, 17862-17871.
- 513 16. W. J. Song, J. Z. Du, T. M. Sun, P. Z. Zhang and J. Wang, *Small*, 2010, **6**, 239-246.
- 514 17. K. A. Fitzgerald, J. F. Guo, E. G. Tierney, C. M. Curtin, M. Malhotra, R. Darcy, F. J.  
515 O'Brien and C. M. O'Driscoll, *Biomaterials*, 2015, **66**, 53-66.
- 516 18. K. Rahme, J. Guo, J. D. Holmes and C. M. O'Driscoll, *Colloids and surfaces. B*,  
517 *Biointerfaces*, 2015, **135**, 604-612.
- 518 19. A. O'Mahony, S. Desgranges, J. Ogier, A. Quinlan, M. Devocelle, R. Darcy, J. Cryan  
519 and C. O'Driscoll, *Pharm Res*, 2013, **30**, 1086-1098.
- 520 20. H. Katas and H. O. Alpar, *Journal of controlled release : official journal of the*  
521 *Controlled Release Society*, 2006, **115**, 216-225.
- 522 21. M. Y. Lee, S. J. Park, K. Park, K. S. Kim, H. Lee and S. K. Hahn, *ACS nano*, 2011, **5**,  
523 6138-6147.
- 524 22. A. Kichler, *The journal of gene medicine*, 2004, **6 Suppl 1**, S3-10.
- 525 23. W. T. Godbey, K. K. Wu and A. G. Mikos, *J Biomed Mater Res*, 1999, **45**, 268-275.
- 526 24. S. Son, R. Namgung, J. Kim, K. Singha and W. J. Kim, *Accounts of chemical*  
527 *research*, 2012, **45**, 1100-1112.
- 528 25. R. Banerjee, P. Tyagi, S. Li and L. Huang, *International journal of cancer. Journal*  
529 *international du cancer*, 2004, **112**, 693-700.

- 530 26. A. Garaikoetxea Arguinzoniz, N. Gomez Blanco, P. Ansorena Legarra and J. C.  
531 Mareque-Rivas, *Dalton transactions*, 2015, **44**, 7135-7138.
- 532 27. Y. Lee, S. H. Lee, J. S. Kim, A. Maruyama, X. S. Chen and T. G. Park, *Journal of*  
533 *Controlled Release*, 2011, **155**, 3-10.
- 534 28. K. Sun, J. X. Qiu, J. W. Liu and Y. Q. Miao, *J Mater Sci*, 2009, **44**, 754-758.
- 535 29. H. Tyagi, A. Kushwaha, A. Kumar and M. Aslam, *International Journal of*  
536 *Nanoscience*, 2011, **10**, 857-860.
- 537 30. X. Huang, P. K. Jain, I. H. El-Sayed and M. A. El-Sayed, *Nanomedicine*, 2007, **2**,  
538 681-693.
- 539 31. W. Xu, J. Y. Park, K. Kattel, M. W. Ahmad, B. A. Bony, W. C. Heo, S. Jin, J. W.  
540 Park, Y. Chang, T. J. Kim, J. A. Park, J. Y. Do, K. S. Chae and G. H. Lee, *Rsc Adv*,  
541 2012, **2**, 10907-10915.
- 542 32. A. F. M. El-Mahdy, T. Shibata, T. Kabashima, Q. C. Zhu and M. Kai, *Rsc Adv*, 2015,  
543 **5**, 32775-32785.
- 544 33. N. S. Gandhi, R. K. Tekade and M. B. Chougule, *Journal of controlled release :*  
545 *official journal of the Controlled Release Society*, 2014, **194**, 238-256.
- 546 34. A. M. O'Mahony, J. Ogier, R. Darcy, J. F. Cryan and C. M. O'Driscoll, *PloS one*,  
547 2013, **8**, e66413.
- 548 35. C. S. John, B. J. Vilner, B. C. Geyer, T. Moody and W. D. Bowen, *Cancer Res*, 1999,  
549 **59**, 4578-4583.
- 550 36. S. D. Li, S. Chono and L. Huang, *Journal of controlled release : official journal of the*  
551 *Controlled Release Society*, 2008, **126**, 77-84.
- 552 37. G. Creusat, A. S. Rinaldi, E. Weiss, R. Elbaghdadi, J. S. Remy, R. Mulherkar and G.  
553 Zuber, *Bioconjugate chemistry*, 2010, **21**, 994-1002.
- 554 38. J. F. Guo, K. Rahme, K. A. Fitzgerald, J. D. Holmes and C. M. O'Driscoll, *Nano Res*,  
555 2015, **8**, 3111-3140.
- 556 39. N. M. Schaeublin, L. K. Braydich-Stolle, A. M. Schrand, J. M. Miller, J. Hutchison, J.  
557 J. Schlager and S. M. Hussain, *Nanoscale*, 2011, **3**, 410-420.
- 558 40. C. M. Goodman, C. D. McCusker, T. Yilmaz and V. M. Rotello, *Bioconjugate*  
559 *chemistry*, 2004, **15**, 897-900.
- 560 41. H. Y. Xue, S. Liu and H. L. Wong, *Nanomedicine*, 2014, **9**, 295-312.
- 561 42. D. Brunner, J. Frank, H. Appl, H. Schoffl, W. Pfaller and G. Gstraunthaler, *Altex*,  
562 2010, **27**, 53-62.
- 563 43. T. S. Hauck, A. A. Ghazani and W. C. Chan, *Small*, 2008, **4**, 153-159.
- 564 44. J. C. Evans, J. McCarthy, C. Torres-Fuentes, J. F. Cryan, J. Ogier, R. Darcy, R. W.  
565 Watson and C. M. O'Driscoll, *Gene therapy*, 2015, **22**, 802-810.
- 566 45. P. C. Patel, D. A. Giljohann, W. L. Daniel, D. Zheng, A. E. Prigodich and C. A.  
567 Mirkin, *Bioconjugate chemistry*, 2010, **21**, 2250-2256.
- 568 46. A. Albanese and W. C. Chan, *ACS nano*, 2011, **5**, 5478-5489.
- 569 47. J. V. Jokerst, T. Lobovkina, R. N. Zare and S. S. Gambhir, *Nanomedicine*, 2011, **6**,  
570 715-728.